

Naruhiro Matsufuji

Abstract

A primary goal for treatment delivery is to achieve a homogenous effect throughout the target volume. In contrast to conventional photon therapy, this cannot be achieved by applying a uniform distribution of absorbed dose within the target volume due to the drastic change in the biological effectiveness of ion beam as shown in the previous section. In this section, biophysical models used in carbon-ion radiotherapy (C-ion RT) at HIMAC are explained.

Keywords

Linear quadratic model • Microdosimetric kinetic model • RBE

5.1 Usage of RBE in Carbon-Ion Radiotherapy

As introduced in Sect. 5.1, the term relative biological effectiveness (RBE) is defined as a concept in radiobiology as the ratio of absorbed dose required to evoke the same biological effect (endpoint) by two different radiations. If this RBE is introduced in clinical situation, the clinical effect (tumor control) is expected to be the same if the RBE-weighted dose is the same. In case of proton therapy, generic RBE of 1.1 has been recommended [1] irrespective of dose-modifying factors of radiation effects such as fractionation, overall time, and tissue type or radiation quality of the therapeutic beams.

C-ion RT is on the same line with this proton RBE usage. There are little evidences for the comparison on the clinical outcomes between X-ray and C-ion RT due to vast difference in target selection, fraction size, schedule, and so on. In this sense that the clinical RBE has not yet been proven in C-ion RT, however, the term RBE is used in this textbook as a dose modification factor from the viewpoint of consistency in notation between proton and C-ion RT.

RBE-weighted absorbed dose, designated by D_{RBE} , represents the product of the ion absorbed dose, D , and the RBE with respect to photons delivered under the same conditions.

$$D_{RBE} = RBE \times D \quad (5.1)$$

where D represents the ion absorbed dose, expressed in gray (Gy). D_{RBE} is the RBE-weighted carbon ion absorbed dose and is the dose of photons that would produce the same therapeutic effect as an ion absorbed dose, D , given under identical circumstances; it is also expressed in gray (Gy). To avoid this confusion the quantity D_{RBE} is expressed in units of Gy, followed by a space and the parenthetical descriptor “(RBE).” The RBE-weighted absorbed dose specification would read “ $D_{RBE} = 70 \text{ Gy (RBE)}$.” This notation will be used throughout the remainder of this textbook. RBE of therapeutic carbon-ion beams can be affected by many factors complexly such as dose level, linear energy transfer (LET), biological endpoint, fractionation, oxygen status, and so on. The role of the biophysical model is to take into account the changeable biological effect appropriately in treatment planning. However, full simulation of the underlying biological processes is not yet feasible the physical properties of the different radiation types can be described in great detail and thus form the basis of different theoretical approaches/models to predict the increased effectiveness of particle beams in experimental and therapeutic situations.

N. Matsufuji (✉)
National Institute of Radiological Sciences, 9-1, Anagawa-4,
Inage-ku, Chiba 263-8555, Japan
e-mail: matufuji@nirs.go.jp

5.2 Biophysical Model in Carbon-Ion Radiotherapy

When starting C-ion RT at HIMAC in 1994, little was known on the clinical effectiveness of ion beams. In order to design the dose distribution under the situation, an experimentally oriented pragmatic approach has been developed [2], referring to the clinical experience with neutron beams and combined with a dose-escalation strategy. Therefore, the estimation of the clinically relevant RBE values is implemented as a two-step procedure in this case, where a “biological RBE” is distinguished from the “clinical RBE.”

The first step includes the shaping of the spread-out Bragg peak (SOBP) and thus the ridge filter design. It is based on similar procedures developed for the pioneering study at LBL, but slightly differs with respect to the endpoints chosen as representative for the typical treatments performed at HIMAC, i.e., a human salivary gland (HSG) tumor cell line was selected as in vitro model system because the initial patients to receive carbon-ion radiotherapy were forecasted to have salivary gland tumors, which were known to respond well to fast neutron therapy.

5.2.1 Shaping of the SOBP

Treatment fields for application in tumor therapy are typically characterized by a superposition of Bragg peaks with different energies and even different ion species. The field is characterized by a distribution of LET values. Therefore, it is of particular interest to determine the RBE as a function of depth in such a typical mixed field treatment configuration. In general, dose-averaged LET value, determined by weighting the individual components of the field by their contribution to the total dose, is regarded as an adequate index for the biological effectiveness of mixed fields. Due to fragmentation of the primary carbon ions, a small dose contribution originating from the lighter particles is observed in the beam and more prominent beyond the distal falloff of the dose distribution. Though the RBE values might differ even in the case of similar dose-averaged LET values if different ion species are contaminated, the influence was regarded limited and therefore negligible in this model.

For the HSG cells, cell survival measurements were performed for different monoenergetic beams and mixed beams [3] covering a broad LET range, from which the linear-quadratic coefficients $\alpha(x)$ and $\beta(x)$ as a function of the depth x in a monoenergetic, pristine Bragg peak can be derived according to the LET at the depth x as shown as Eq. (5.2). Based on these values, dose-effect curves for mixed fields composed of k Bragg peaks were calculated

from the linear-quadratic coefficients $\alpha_{RM}(x)$ and $\beta_{RM}(x)$ at the depth x in a range-modulated Bragg peak by using Eqs. (5.3) and (5.4):

$$S = \exp\{-[\alpha_{RM}(x)d + \beta_{RM}(x)d^2]\} \quad (5.2)$$

$$\alpha_{RM}(x) = \frac{\sum_1^k r_j d(x+s_j) \alpha(x+s_j)}{\sum_1^k r_j d(x+s_j)} \quad (5.3)$$

$$\sqrt{\beta_{RM}(x)} = \frac{\sum_1^k r_j d(x+s_j) \sqrt{\beta(x+s_j)}}{\sum_1^k r_j d(x+s_j)} \quad (5.4)$$

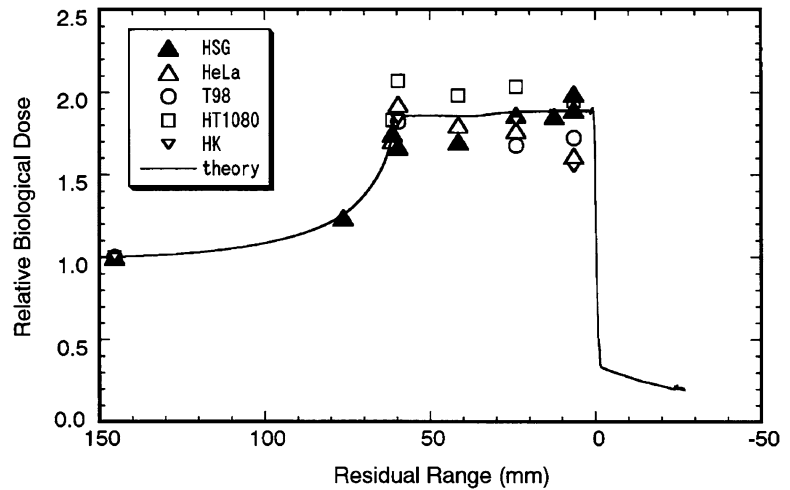
Here, r_j denotes the weight, i.e., the relative fluence contribution, of the j th pristine Bragg peak to the total SOBP, $d(x)$ denotes the dose deposition in depth x of a pristine Bragg peak, and s_j denotes the distance between the position x and the depth of the j th Bragg peak. Using $\alpha_{RM}(x)$ and $\beta_{RM}(x)$, survival at depth x can be determined for the given total dose at that depth, and finally the corresponding biological RBE can be determined.

The 10 % surviving fraction level for HSG cells was chosen as the relevant endpoint for biological RBE determination of carbon ions. This allowed the design of a ridge filter required to achieve a homogenous cell killing of HSG cells throughout the extension of the SOBP. The design has been checked experimentally by irradiation of HSG cells with carbon ions at various positions of a 6-cm SOBP. Figure 5.1 shows the biological RBE-weighted dose distribution of 290 MeV/n carbon-ion beams with a 6-cm SOBP [3]. The biological RBE-weighted doses range from 1.6 to 2.1 Gy (RBE) within the SOBP, depending on cell lines and positions. HT1080 cells show slightly higher RBE-weighted doses than HSG cells at proximal positions while the reverse is true at distal positions. In general, however, the biological dose distributions are sufficiently flat. Because they were derived from in vitro cell survival data, the corresponding RBE values were designated “biological RBE.”

5.2.2 Determination of Neutron Equivalent Point

In a second step, the link to previous experience with neutron therapy was made. Biological RBE values of neutrons for cultured cells and in vivo systems are experimentally obtainable and can be compared with RBE values of carbon ions. A position in the SOBP was determined which exhibited the same biological RBE as the neutron radiation used for the

Fig. 5.1 Biological dose distribution of a therapeutic carbon beam. The Bragg peak of a monoenergetic carbon beam of 290 MeV/n was spread out to 6 cm. Image from published paper [3]



clinical trials at NIRS. This position is designated the “neutron equivalent point” in the SOBP. Measurements of the biological RBE for 10 % cell survival of HSG cells revealed that after irradiation within a 6-cm SOBP the RBE increased with an increase of dose-averaged LET of carbon ions and was 2.05 at 85 keV/μm (see Fig. 5.2 [3]). This RBE was identical to the neutron RBE for the same endpoint. Similar measurements were performed for normal tissue effects in an in vivo system, where RBE for the induction of early skin reaction was determined at a scoring level of 2.5 (dry desquamation) as endpoint. Here, the RBE of 3.1—corresponding to the neutron RBE—was achieved at a dose-averaged LET of 75 keV/μm for carbon ions. Combining the results for in vitro and in vivo systems, it was thus decided to use the point with an LET of 80 keV/μm as the neutron equivalent point; this corresponds to a position approximately 8 mm upstream of the distal falloff in case of the 6-cm SOBP with 290 MeV/n beam.

Therefore, it was assumed that the RBE at this position of a carbon-ion SOBP should be the same as that of fast neutrons used for patient therapy. The NIRS experience of fast neutron therapy in the past was thus used to determine the corresponding “clinical RBE” of carbon-ion therapy at one point in the SOBP.

5.2.3 Estimation of Clinically Applicable RBE-Weighted Dose Profile

Tsunemoto [4] published clinical results of fast neutron therapy at NIRS. He summarized clinical results after various fractionation schedules for fast neutron therapy. Kutsutani-Nakamura [5] published a treatment planning method of fast neutron therapy and calculated RBE values of fast neutrons for tolerance of acute skin reaction. Based on the formula $RBE(N) = 1.8 \times N^{0.2}$, he calculated clinical RBE values of

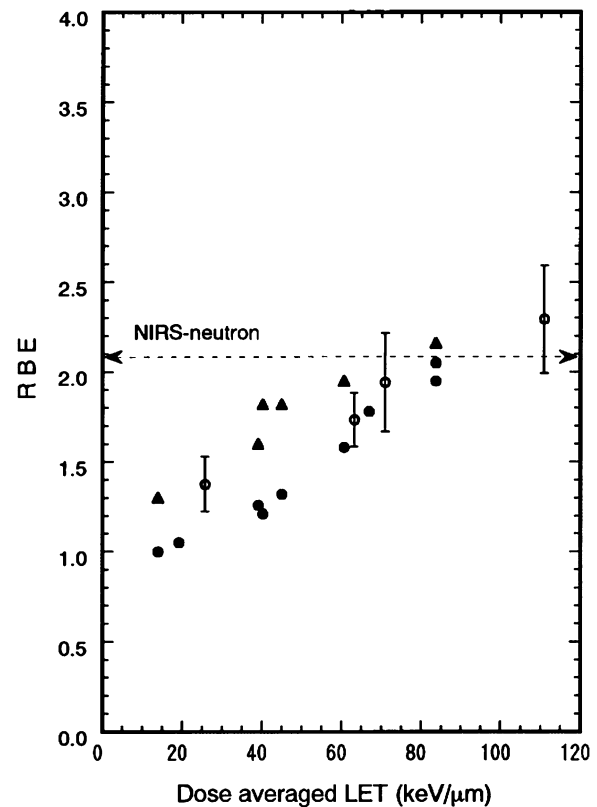


Fig. 5.2 LET dependency of the RBE for colony formation of HSG cells at the 10 % survival level. The data of the RBE were obtained by exposures of a HIMAC carbon beam of 290 MeV/n. The dashed line shows the RBE for the NIRS neutron beam for the HSG cells. Image from published paper [3]

neutron vs. number of fraction (N). Depending on the number of fractions the clinical RBE of neutrons increased such that it was 2.5, 2.9, and 3.3 as the number of fractions increased from 5, 10, and 20. Because it was intended to use an 18-fraction scheme over 6 weeks for C-ion RT, which is

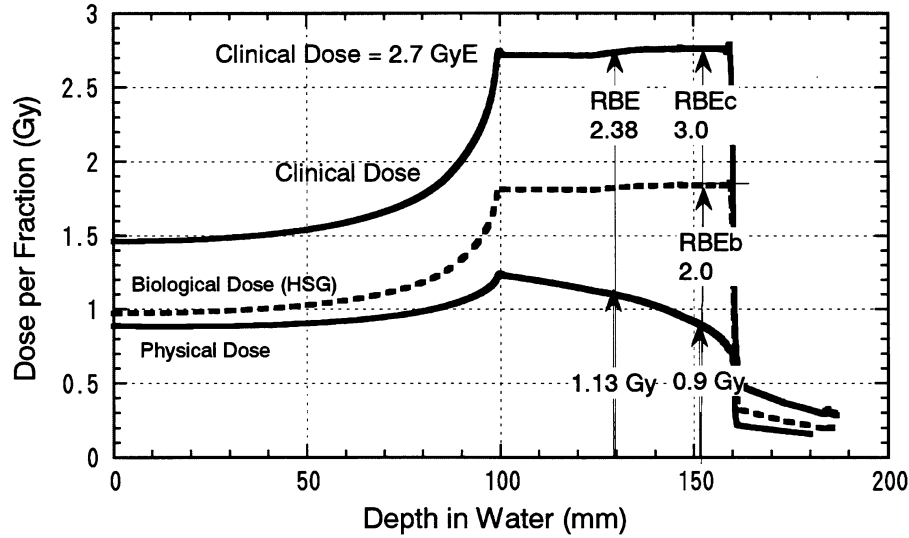


Fig. 5.3 Schematic method used to determine the RBE at the center of the SOBP for the clinical situation. Image from published paper [3]

slightly different from the schemes used for neutron irradiation, a value of 3.0 was selected for the neutron RBE.

In order to move from a biological endpoint to a clinical endpoint it was assumed that a flat RBE-weighted dose distribution for one endpoint can be transformed into a flat RBE-weighted dose distribution of a different endpoint by appropriate scaling with a single value. According to this approximation, the so-called clinical dose distribution can be obtained by scaling the RBE-weighted dose distribution for in vitro cell survival by the conversion factor between the clinically observed RBE values for neutron radiation and the RBE for HSG cell survival at the neutron equivalent point.

In the example given in Fig. 5.3 [3], a clinical RBE-weighted dose of 2.7 Gy (RBE) would be given at any position within the SOBP. According to the assumed neutron RBE of 3, this requires an absorbed dose of 0.9 Gy at the neutron equivalent point 8 mm upstream of the distal end of the carbon SOBP. The biological RBE for 10 % HSG cell survival at this position is 2.0. The assumed RBE for the clinically applicable RBE-weighted dose distribution is then obtained by scaling the RBE-weighted dose profile for the HSG cell survival by a common scaling factor of $3.0/2.0=1.5$ at each position in the field. The resulting RBE values for any position are then obtained by comparing this scaled profile with the absorbed dose profile;

for example, at the middle of SOBP, based on an absorbed dose of 1.13 Gy, an RBE of $2.7/1.13=2.4$ is estimated.

5.2.4 Validity of the Model

The clinical validation of the underlying RBE model needs to be performed systematically using the clinical data derived from the dose-escalation studies. We present here the tumor control probability (TCP) analysis for non-small cell lung cancer (NSCLC) as an example for the validation of the clinical results in terms of the abovementioned clinical RBE prescription scheme.

Miyamoto et al. [6] analyzed the clinical results of NSCLC treated by HIMAC beams. They depicted a very conspicuous dose dependency of the local control rate. A dose-escalation study was performed with a treatment schedule of 18 fractions in 6 weeks. Hayakawa et al. reported the local control rate for NSCLC using photons. In order to compare the two results, dose dependency of TCP with the photon beam was fitted by the following formula [7]:

$$TCP = \sum \frac{1}{\sqrt{2\pi\sigma}} \exp\left[-\frac{(\alpha_i - \alpha)^2}{2\sigma^2}\right] \cdot TCP(\alpha_i) \quad (5.5)$$

$$TCP(\alpha_i) = \exp\left\{-N \exp\left[-n\alpha_i d \left(1 + \frac{d}{\alpha_i/\beta}\right) + \frac{0.693(T - T_k)}{T_d}\right]\right\} \quad (5.6)$$

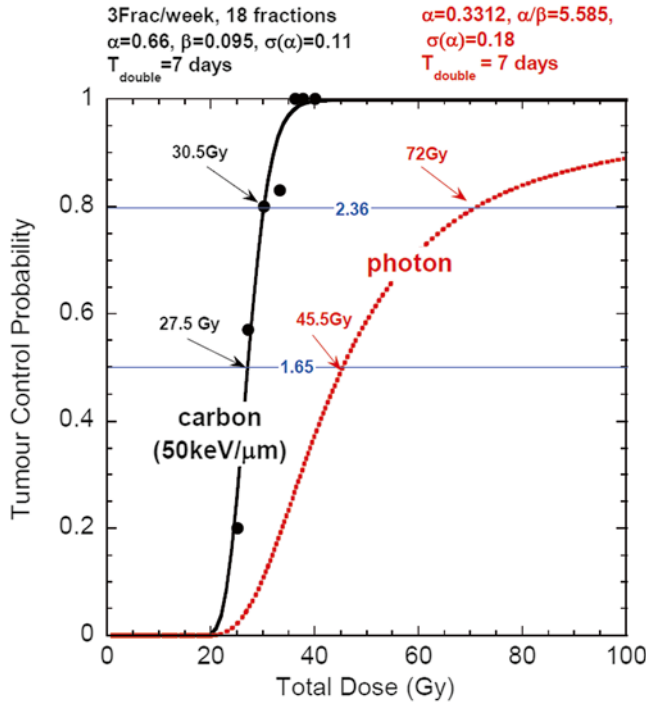


Fig. 5.4 TCP of NSCLC with photon (dashed, red line) and carbon (black line) beams. Circles show clinical results at HIMAC. For carbon TCP, the width of SOBP and LET were fixed at 60 mm and 50 keV/μm, respectively. Image from published paper [8]

α and β are coefficients of the linear-quadratic (LQ) model of the cell survival curve. In the analysis, α and β values of HSG cells were used. σ is a standard deviation of the coefficient α , which reflects patient-to-patient variation of radiosensitivity. N is the number of clonogens in tumor (fixed value of 10^9 was used). n and d are total fraction number and the fractionated dose, respectively. T (42 days), T_k (0 day), and T_p (7 days) are overall time for treatment, kick-off time, and average doubling time of tumor cells, respectively. Values used in the analysis are shown in brackets. The result is shown in Fig. 5.4 [8].

The same analysis was carried out to determine the TCP using carbon-ion RT [9]. Here, the width of SOBP and dose-averaged LET in the SOBP region were both fixed at 60 mm and 50 keV/μm, respectively, for simplicity. The result is also shown in Fig. 5.4. It is clear from the figure that the TCP curve of the carbon beam is much steeper than that of the photon beam. The value of σ in Eq. (5.5) was 0.18 for the photon beam, while that for the carbon beam was reduced to 0.11. The result implies that carbon beam provides equally excellent local tumor control regardless of the individual radiosensitivity.

Taking into account the difference between the TCP slopes shown in Fig. 5.4 when TCP is regarded as an endpoint, the RBE value is found to be dependent on the TCP level. Furthermore, the biological RBE value coincided with the RBE at 50 % TCP, whereas the clinical RBE value corresponded to that at 80 % TCP [8]. This agreement of the designed clinical RBE at higher TCP level is considered to be justified from the therapeutic point of view.

5.2.5 Characteristics of NIRS RBE

In the clinical trial of hypo-fractionation and dose-escalation studies of ion beam therapy, the number of fractions was decreased and the dose per fraction increased. The biological RBE of the treatment beam increases according to the dose level treated. However at NIRS a constant dose-weighting factor is assumed, independent of dose per fraction. From the definition of RBE, which is biological effectiveness relative to 250 KV X-ray, this is apparently a contradictory usage of the term ‘‘RBE.’’ Nevertheless this framework is worth for treatments restricted to the use of ion beams only. Here, RBE in NIRS approach is not the one referring equivalency to photon therapy but the one used to express the weighting factor.

The principle of depth-clinical dose profile used at NIRS can be summarized as Eq. (5.7).

$$D_{CRx}(z) = 1.45 \times \frac{d_x^{HSG}(0.1)}{d_{SOBP}^{HSG}(0.1; z)} \times D(z; SOBP; E) = CRx(z; SOBP; E) \times D(z; SOBP; E) \quad (5.7)$$

$$D_{CRx}(z; SOBP; E) = 1.45 \times \frac{d_x^{HSG}(0.1)}{d_{SOBP}^{HSG}(0.1; center)} \times \frac{d_x^{HSG}(0.1; center)}{d_{SOBP}^{HSG}(0.1; z)} \quad (5.8)$$

where the number 1.45 is the ratio of clinical RBE used in the NIRS neutron therapy and the biological RBE of HSG for the neutron beam. $D(z; SOBP, E)$ is the physical dose of SOBP beam at depth of z for the initial energy of E . $d_x^{HSG}(0.1)$

and $d_{SOBP}^{HSG}(0.1; z)$ are a physical dose of photon and SOBP carbon beam at depth of z which are required to achieve the survival fraction of 10 % for HSG cells, respectively. In the NIRS approximation, the shapes of the physical dose

distribution of the SOBP are assumed to be fixed regardless of the dose level.

$$\frac{d_{SOBP}^{HSG}(0.1;center)}{d_{SOBP}^{HSG}(0.1;z)} \approx \frac{d_x^{HSG}(s;center)}{d_{SOBP}^{HSG}(s;z)} \quad (5.9)$$

From the above approximation, RBE is not dependent on the dose level to be treated. The optimized dose of carbon therapy has been clinically obtained through dose-escalation studies of clinical trial of carbon therapy at NIRS.

5.3 Improvement of the Biophysical Model

For a given ion species and cell type, as the first approximation LET or dose-averaged LET is a good predictor for the RBE. However, when comparing different ion species, LET is not flawless in a strict sense to uniquely describe the RBE. This can be attributed to the fact that LET is a simplified one-dimensional representation of the particle track, which does not take into account the three-dimensional distribution of energy deposition around the particle trajectory. Since for a given LET value the corresponding energy is lower for a light particle as compared to a heavier particle, the track radius is smaller for the lighter particle because of the lower energy transferred to the secondary electrons. As a consequence, the average energy density is higher in the track of the light particle, finally leading to the higher effectiveness. This problem made it necessary in the original model to tabulate α and β parameters in the LQ model as functions of ion species and energy. Pragmatically this works fairly well in most conditions; however, it is inevitable to introduce a kind of assumption or interpolation at a condition out of the table. Eventually it could not only introduce a possible error in the estimation of therapeutic effectiveness of carbon ions, but also it makes it difficult to make a prospective, reliable, or mechanistic estimation of the beam. In order to account for that, upon the accumulated knowledge in the first decade, we aimed at updating the biophysical model in more mechanistic approach for the biological effect of ion beams which leads to thorough understanding of the clinical effectiveness of the ion beams designed with the original pragmatic approach.

Methods based on microdosimetric characterization of the radiation field focus on a detailed description of the stochastic energy deposition distributions. Experimental microdosimetry is based on measurements or calculation of energy deposition events typically in spherical volumes of simulated micrometer dimensions. Microdosimetric kinetic model (MKM) has been developed by Hawkins [10] as a model to predict biological effectiveness of radiations based on the microscopic spatial energy distribution. MKM real-

izes prospective estimation of biological effectiveness of various ion species based on their physical properties. This is expected to provide more precise estimation of the biological effectiveness of the therapeutic carbon beam; therefore, MKM has been introduced as the updated biophysical model implemented in the new treatment planning system for scanning irradiation.

MKM extended the microdosimetric concept of the theory of dual radiation action (TDRA) [11], which gives estimation of biological effect based on the energy deposited in a site in the order of micrometer. In TDRA, the number of lesion L is proportional to the square of the specific energy z given in the site while MKM incorporates additional component in lesion formation which is linearly proportional to the specific energy as

$$L = Az + Bz^2 \quad (5.10)$$

The units for y are the same as for the LET, namely keV/ μm . Similar to the LET, also for the lineal energy, the dose-weighted average value y_D is expected to be representative for the biological effectiveness:

$$-\ln S = N\bar{L} = N(A\bar{z} + B\bar{z}^2) = (\alpha_0 + \beta \cdot z_{1D}) + \beta D^2 \quad (5.11)$$

where α_0 denotes the initial slope of the survival curve in the limit $\text{LET} \rightarrow 0$ and β is assumed to be independent on radiation quality. Since z_{1D} rises with LET, Eq. (5.9) would lead to a steady increase of RBE with LET. However, RBE is known to decrease with LET after reaching a maximum at approximately 100 keV/ μm . Therefore, saturation correction on specific energy was introduced [12].

$$z_{1D}^* = \frac{l}{m} y_0^2 \cdot \frac{\int [1 - \exp(-y^2/y_0^2)] f(y) dy}{\int y f(y) dy} \quad (5.12)$$

By replacing z_{1D} in Eq. (5.9) with z_{1D}^* , the modified MKM is shown to allow a good representation of the experimental data. Figure 5.5 [12] shows the experimental α value of HSG cells for various incident beams as a function of its saturation-corrected lineal energy. As demonstrated in the figure, this saturation-corrected modified MKM is useful in estimating the biological effectiveness of various ion species. The modified MKM has been installed in the treatment planning both for scanning irradiation [13] and broad-beam irradiation.

Figure 5.6 shows the cell survival distribution of HSG cells for the beam of C-290 MeV/n with 60 mm SOBP. As shown in the figure, MKM can predict the HSG cell response in excellent precision. Figure 5.7 shows the comparison of depth-biological dose profile for the beam in Fig. 5.6 with the original model (labeled as KANAI1999 in the figure) and MKM. Both models agreed to each other in general. This proves that the original approach is

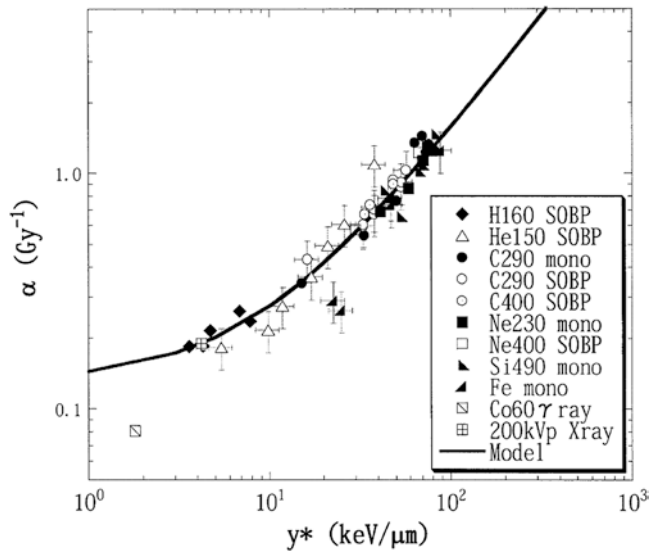


Fig. 5.5 Experimental α value with $\beta=0.05 \text{ Gy}^{-2}$ fixed for HSG cells as a function of the saturation-corrected dose mean lineal energy, y^* . The values of y^* were measured by the TEPC with a simulated diameter of $1.0 \mu\text{m}$ and with a saturation parameter of $y_0=150 \text{ keV}/\mu\text{m}$. The solid line indicates the curve calculated using saturation-corrected modified MKM. Image from published paper [12]

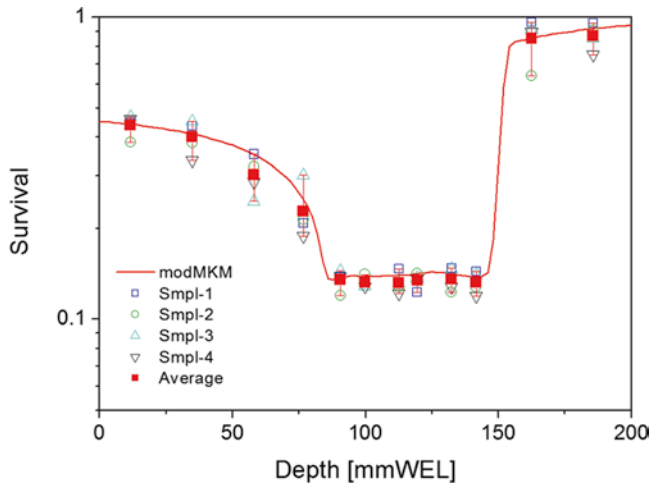


Fig. 5.6 Cell survival distribution of HSG cells for the beam of C-290 MeV/n with 60 mm SOBP. The beam is delivered by scanning method at HIMAC. Line in the figure shows the estimation of MKM

pragmatically adequate enough for the therapeutic purpose. Slight difference found at the distal part of the SOBP can be attributed to the improved estimation of the MKM on the biological effect of the beam where the fragment particles are relatively abundant.

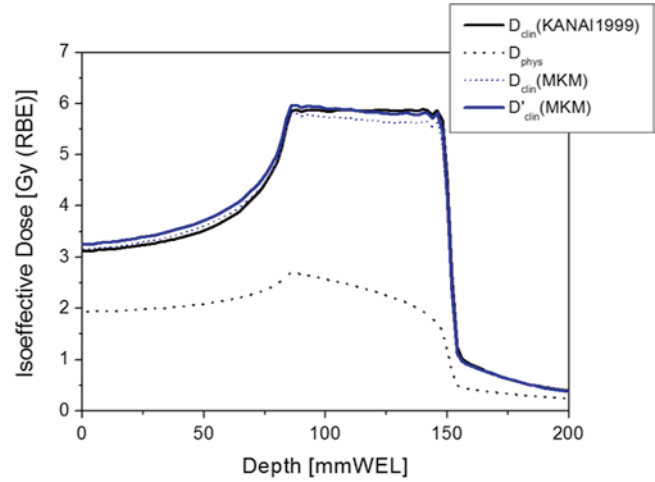


Fig. 5.7 Depth-biological dose profile corresponding to Fig. 5.6

References

1. International Commission on Radiation Units & Measurements. Prescribing, recording, and reporting proton-beam therapy (ICRU Report 78). Maryland: Bethesda; 2009.
2. Kanai T, Endo M, Minohara S, et al. Biophysical characteristics of HIMAC clinical irradiation system for heavy-ion radiation therapy. *Int J Radiat Oncol.* 1999;44:201–10.
3. Kanai T, Furusawa T, Fukutsu K, et al. Irradiation of mixed beam and design of spread-out Bragg peak for heavy-ion radiotherapy. *Radiat Res.* 1997;147:78–85.
4. Tsunemoto H. Clinical evaluation of fast neutron therapy. *Nippon Igaku Hoshasen Gakkai Zasshi.* 1982;42:823–47.
5. Kutsutani-Nakamura Y. Treatment planning method in the use of the TDF biological equivalent concept in fast neutron therapy. *Nippon Igaku Hoshasen Gakkai Zasshi.* 1978;38:950–60.
6. Miyamoto T, Yamamoto N, Nishimura H, et al. Carbon ion radiotherapy for stage I non-small cell lung cancer. *Radiother Oncol.* 2003;66:127–40.
7. Webb S, Nahum AE. A model for calculating tumour control probability in radiotherapy including the effects of inhomogeneous distributions of dose and clonogenic cell density. *Phys Med Biol.* 1993;38:653–66.
8. Matsufuji N, Kanai T, Kanematsu N, et al. Specification of carbon ion dose at the National Institute of Radiological Sciences (NIRS). *J Radiat Res.* 2007;48:A81–6.
9. Kanai T, Matsufuji N, Miyamoto T, et al. Examination of GyE system for HIMAC carbon therapy. *Int J Radiat Oncol.* 2006;64:650–6.
10. Hawkins RB. A statistical theory of cell killing by radiation of varying linear energy transfer. *Radiat Res.* 1994;140:346–67.
11. Kellerer AM, Rossi HH. A generalized formation of dual radiation action. *Radiat Res.* 1978;75:471–88.
12. Kase Y, Kanai T, Matsumoto M, et al. Microdosimetric measurements and estimation of human cell survival for heavy-ion beams. *Radiat Res.* 2006;166:629–38.
13. Inaniwa T, Furukawa T, Kase Y, Matsufuji N, Toshito T, Matsumoto Y, Furusawa Y, Noda K. Treatment planning for a scanned carbon beam with a modified microdosimetric kinetic model. *Phys Med Biol.* 2010;55:6721–37.